Hindawi Publishing Corporation
International Journal of Antennas and Propagation
Volume 2015, Article ID 971646, 9 pages
http://dx.doi.org/10.1155/2015/971646

Research Article

Optimization and Design of Wideband Antenna Based on Q Factor

Han Liu,[1] Chengyou Yin,[1] Weidong Gao,[1] and Yulong Sun[2]

[1]*Hefei Electronic Engineering Institute, 460 Huangshan Road, Hefei, Anhui 230037, China*
[2]*Shengli Oilfield Company, SINOPEC, 483 Xisi Road, Dongying, Shandong 257051, China*

Correspondence should be addressed to Han Liu; lujiangliuhan@sina.com

Received 3 September 2015; Revised 5 November 2015; Accepted 9 November 2015

Academic Editor: Miguel Ferrando Bataller

A wideband antenna is designed based on Q factor in this paper. Firstly, the volume-surface integral equations (VSIEs) and self-adaptive differential evolution algorithm (DEA) are introduced as the basic theories to optimize antennas. Secondly, we study the computation of Q of arbitrary shaped structures, aiming at designing an antenna with maximum bandwidth by minimizing the Q of the antenna. This method is much more efficient for only Q values at specific frequency points that are computed, which avoids optimizing bandwidth directly. Thirdly, an integrated method combining the above method with VSIEs and self-adaptive DEA is employed to optimize the wideband antenna, extending its bandwidth from 11.5~16.5 GHz to 7~20 GHz. Lastly, the optimized antenna is fabricated and measured. The measured results are consistent with the simulated results, demonstrating the feasibility and effectiveness of the proposed method.

1. Introduction

Wideband communication systems have been drawing considerable attention among researchers and the industrial community due to the advantages provided by them such as high data rate, compact system size, and low power consumption. Antenna is an indispensable component of any wireless device. The optimal performance of a radio system depends greatly on efficient design of the antenna. So the research of wideband antennas has become a hot topic [1]. Many researchers have designed varieties of ultra-wideband (UWB) antennas with good performance in recent years. Samal et al. [2] proposed an UWB all-text antenna with full ground plane for off-body wireless body area networks (WBAN) applications. The key innovation of the proposed antenna is the use of the quite large and full ground plane, which avoids coupling to and consequently power absorption by the human body. As wideband antenna theory is not yet mature, its design is mostly based on experience with simulation software, which wastes much time. There are some researchers who have tried to design wideband antenna with numerical approaches and optimization algorithms. Ou et al. [3] proposed a method combining genetic algorithm (GA) and the method of moments (MoM) to optimize wideband antenna. The method operates in frequency domain and frequency range to be optimized is so large that there are too many S_{11} that should be calculated, which costs too much time. Kim et al. [4] optimized an UWB antenna based on GA and finite-difference time-domain (FDTD). However, codes of FDTD are complicated and FDTD is based on difference operation, which has low accuracy compared with MoM. As a result, we should seek for more effective ways to design wideband antennas. We can find that Q factor is related to size of the antenna. The greater size the antenna occupies, the smaller Q the antenna has. Additionally, antenna bandwidth is also related to Q factor. The smaller the Q is, the wider the antenna bandwidth is. Therefore, we can infer the reduction of antenna size and the increase of bandwidth is contradictory in the process of antenna design. In this paper, we attempt to achieve the following goals. (1) The size of fabricated antenna is as small as possible [5, 6]. (2) The desired antenna bandwidth is as wide as possible. For the above purposes, we

have two alternative resolutions: one is designing an antenna with maximum bandwidth in the case that antenna volume meets system requirements and the other is designing an antenna with minimum volume in the case that antenna performance meets system requirements. This paper will start with the first resolution to increase antenna bandwidth by optimizing Q factor.

The remainder of this paper is organized as follows. In Section 2, the basic theories, including the volume-surface integral equations (VSIEs) and self-adaptive differential evolution algorithm (DEA), are introduced. Q factor of arbitrary shaped structures is studied in Section 3. A wideband antenna is designed based on Q factor in Section 4. Finally, Section 5 is the conclusion.

2. Basic Theory

2.1. The Volume-Surface Integral Equations. Integral equation approach has been widely employed to solve electromagnetic (EM) problems due to its unique merits compared with other numerical approaches like FDTD and finite element method (FEM). Closed-form spatial domain Green's function can be used to study microstrip antennas with infinite ground plane [7]. However, this method cannot work for antennas with finite ground plane. For microstrip antennas, the patch can be processed by surface integral equation and the substrate can be processed by volume integral equation. Therefore, the VSIEs, with high computational accuracy, can be used to analyze any antenna with arbitrary shape.

Assuming there is an antenna that contains perfectly conducting surfaces S and dielectric volumes V, there are N RWG basis functions and M SWG basis functions; the matrix equation based on the MoM can be expressed as

$$\mathbf{ZI} = \mathbf{V}, \tag{1}$$

where

$$\mathbf{V} = \begin{bmatrix} V_1 \\ V_2 \end{bmatrix} = \begin{bmatrix} \left[\left\langle \mathbf{E}^i, \mathbf{f}_m \right\rangle\right]_{m=1,\ldots,N} \\ \left[\left\langle \mathbf{E}^i, \mathbf{q}_m \right\rangle\right]_{m=1,\ldots,M} \end{bmatrix}, \tag{2}$$

$$\mathbf{Z} = \begin{bmatrix} \left[\mathbf{Z}_{\mathrm{cc}_{mn}}\right]_{m,n=1,\ldots,N} & \left[\mathbf{Z}_{\mathrm{cd}_{mn}}\right]_{m=1,\ldots,N,n=1,\ldots,M} \\ \left[\mathbf{Z}_{\mathrm{dc}_{mn}}\right]_{m=1,\ldots,M,n=1,\ldots,N} & \left[\mathbf{Z}_{\mathrm{dd}_{mn}}\right]_{m,n=1,\ldots,M} \end{bmatrix}, \tag{3}$$

$$\mathbf{I} = \begin{bmatrix} \left[I_n\right]_{n=1,\ldots,N} \\ \left[D_n\right]_{n=1,\ldots,M} \end{bmatrix}, \tag{4}$$

where $\mathbf{q}_m$ is the mth SWG basis function and $\mathbf{f}_m$ is the mth RWG basis function. The subscripts c (conductor) and d (dielectric) in (3) are used to represent that the source or test basis function is on conductor and in dielectric, respectively. For example, $\mathbf{Z}_{\mathrm{cd}}$ represents interactions between conductor and dielectric.

With the establishment of the mother impedance matrix, antenna performance can be analyzed through the MATLAB programming based on the VSIEs [8].

2.2. Self-Adaptive Differential Evolution Algorithm. In this paper, the MoM is employed to analyze the antenna, so an optimization algorithm is needed to design the antenna combined with the MoM. DEA, one of the fastest optimization algorithms, has many advantages such as simple process, good robustness, and fast convergence. Parameters of DEA only need to be set once and these parameters can be reused in other cases [9, 10]. The optimization of antenna structures is generally focused on the retention or removal of antenna grids that binary coding is corresponding to. As standard DEA is real coding, we need to convert it to binary coding. The process of binary coding self-adaptive DEA, which is used to optimize antenna structures, is explained as follows.

2.2.1. Initialization. A population should be initialized randomly at the beginning of adaptive DEA, which consists of NP vectors. Each vector represents a possible solution corresponding to a kind of antenna structure. It can be expressed as

$$\mathbf{X}_{i,G} \quad (i = 1, 2, \ldots, NP), \tag{5}$$

where i is the vector number and G is the generation number.

2.2.2. Mutation Operation. The mutation vector in standard DEA can be obtained by

$$\mathbf{V}_{i,G+1} = \mathbf{X}_{r1,G} + \mathbf{F}\left(\mathbf{X}_{r2,G} - \mathbf{X}_{r3,G}\right). \tag{6}$$

In (6), $r1$, $r2$, and $r3$ are randomly chosen indices from the population and $\mathbf{F}$ is the mutation control parameter. In binary coding DEA, the mutation vector can be expressed as

$$\mathbf{V}_{i,G+1} = \mathbf{X}_{r1,G} + \mathbf{F} \otimes \left(\mathbf{X}_{r2,G} \oplus \mathbf{X}_{r3,G}\right) \quad r_1 \neq r_2 \neq r_3 \neq i, \tag{7}$$

where "+" is "OR" operator, "⊗" is "AND" operator, and "⊕" is "XOR" operator. Each element in $\mathbf{F}$ is 1 or 0 with certain probability.

2.2.3. Crossover Operation. In order to increase the diversity of population, crossover operation is carried out. Trial vectors become

$$\mathbf{U}_{i,G+1} = \left(u_{1i,G+1}, u_{2i,G+1}, \ldots, u_{Di,G+1}\right), \tag{8}$$

$$u_{ji,G+1} = \begin{cases} v_{ji,G+1}, & \text{if } \left(\operatorname{rand} b\left(j\right) \leq \mathrm{CR}\right) \\ x_{ji,G}, & \text{else} \end{cases} \tag{9}$$

$$\left(i = 1, 2, \ldots, NP;\ j = 1, 2, \ldots, D\right).$$

In (9), D is length of code, $\operatorname{rand} b(j)$ is a number from a uniform random distribution within $[0, 1]$, and CR is the crossover index within $[0, 1]$.

In order to avoid the premature convergence and enhance local search ability, CR can be set associated with generation [11], which can be defined as

$$\mathrm{CR} = \mathrm{CR}_{\max} - \frac{t}{T}\left(\mathrm{CR}_{\max} - \mathrm{CR}_{\min}\right), \tag{10}$$

where $\mathrm{CR}_{\max}$ and $\mathrm{CR}_{\min}$ are the upper and lower limits of CR set according to the actual question. t is the current generation, and T is the maximum generation.

2.2.4. Selection Operation. The offspring vector replaces the father vector only when it produces a higher value than the father vector in the next generation, which can be expressed as

$$\mathbf{X}_{i,G+1} = \begin{cases} \mathbf{U}_{i,G+1}, & f(\mathbf{U}_{i,G+1}) > f(\mathbf{X}_{i,G}) \\ \mathbf{X}_{i,G}, & f(\mathbf{U}_{i,G+1}) \le f(\mathbf{X}_{i,G}), \end{cases} \tag{11}$$

where $f(\mathbf{U}_{i,G+1})$, $f(\mathbf{X}_{i,G})$ are the fitness values of the offspring and father vector, respectively.

3. Q Factor of Arbitrary Shaped Structures

Kenneth S. Johnson, the first person to propose the concept of Q factor, defined Q as the ratio of inductance value to resistance value. Chu [12] used spherical waves to express the stored and radiated energies outside the smallest circumscribing sphere of an antenna structure, and the approach has dominated the research on small antennas and offers many results on Q factor. This theory was later extended by Harrington [13] to include circularly polarized antennas and Q is expressed as

$$Q = \frac{1 + 2(kR)^2}{(kR)^3\left[1 + (kR)^2\right]} = \frac{f_c}{BW}. \tag{12}$$

After that, McLean [14] reexamined the case of small antennas [15] and expressed Q as

$$Q = \frac{2\omega W_e}{P_{\text{rad}}} = \frac{1}{(kR)^3} + \frac{1}{kR}. \tag{13}$$

Earlier works [12–14] do not consider actual current distribution, so they have to deal only with bounds related to dimensions of the enclosing sphere. What is more, the results obtained by Chu use a lot of approximations. Therefore, earlier work have limitation in guiding the design of antennas with theoretical minimum Q or minimum size.

In recent years, Thal Jr. [16] and Jelinek et al. [17] have considered the energy in the circumscribing sphere, who figured out new radiation Q limits. As the Jelinek bound is only correct when $ka < 0.5$, it may not be effective in the case of high frequency or antennas with big size.

Many other authors have followed the same paths and given Q of any radiator under different circumstances [18]. But in general, computation of Q is focused on narrow band antennas, which has limitation in guiding the study of wideband antennas.

Q factor is applied to the computation of a wideband antenna in this paper. In order to introduce Q factor to the case of wideband antennas [19, 20], we need to start with the most primitive expression of Q factor. According to related literature [21], for arbitrary radiator, the expression of Q can be written as

$$Q = \frac{2\omega_0 \max\{W_e, W_m\}}{P_{\text{rad}}}. \tag{14}$$

In order to compute antenna Q, it is required to obtain the radiated power P_{rad}, time-average stored electric energy W_e, and time-average stored magnetic energy W_m. By using the method in [22], we can obtain

$$P_{\text{rad}} = \frac{1}{8\pi\omega\varepsilon_0}\int_{V_1}\int_{V_2}\left(k_0^2(\mathbf{J}_1\cdot\mathbf{J}_2^*) - (\nabla_1\cdot\mathbf{J}_1)\cdot(\nabla_2\cdot\mathbf{J}_2^*)\right) \cdot \frac{\sin(k_0 r_{21})}{r_{21}} dV_1 dV_2, \tag{15}$$

$$W_e = \frac{1}{16\pi\omega^2\varepsilon_0}\cdot\left(\int_{V_1}\int_{V_2}(\nabla_1\cdot\mathbf{J}_1)\cdot(\nabla_2\cdot\mathbf{J}_2^*) \cdot \frac{\cos(k_0 r_{21})}{r_{21}} dV_1 dV_2 - \frac{k_0^2}{2} \cdot \int_{V_1}\int_{V_2}\left(k_0^2(\mathbf{J}_1\cdot\mathbf{J}_2^*) - (\nabla_1\cdot\mathbf{J}_1)\cdot(\nabla_2\cdot\mathbf{J}_2^*)\right) \cdot \sin(k_0 r_{21})\, dV_1 dV_2\right), \tag{16}$$

$$W_m = \frac{1}{16\pi\omega^2\varepsilon_0}\cdot\left(k_0^2\int_{V_1}\int_{V_2}(\mathbf{J}_1\cdot\mathbf{J}_2^*) \cdot \frac{\cos(k_0 r_{21})}{r_{21}} dV_1 dV_2 - \frac{k_0}{2} \cdot \int_{V_1}\int_{V_2}\left(k_0^2(\mathbf{J}_1\cdot\mathbf{J}_2^*) - (\nabla_1\cdot\mathbf{J}_1)\cdot(\nabla_2\cdot\mathbf{J}_2^*)\right) \cdot \sin(k_0 r_{21})\, dV_1 dV_2\right). \tag{17}$$

The strict expression of Q, obtained by the above computation, can be used in any radiator. Antenna Q is inversely proportional to bandwidth only for small, high Q, single-resonant antennas [23], and the ratio of the stored energy to the lost energy per one cycle is not uniquely proportional to the fractional bandwidth [24]. For single Q at resonant frequency, the expression above is correct, but in this paper we focus on wideband antenna, and the optimization is on the sum of Q. The relation between the sum of Q and antenna bandwidth is complex. In a word, with the increase of the sum of Q, antenna bandwidth becomes narrow.

Generally speaking, we can optimize S_{11} directly to obtain an antenna with specific bandwidth. But for wideband antennas, the optimization range of bandwidth is so large that S_{11} at too many frequency points should be computed. If the maximum bandwidth is required, the optimization range of the frequency band may not be enough and the optimization range needs to be increasingly expanded. Therefore, the maximum bandwidth cannot be obtained by direct optimization on bandwidth, which can only meet the requirements of specific frequency band. If Q factor is used as optimization function, the problem above will be easily solved.

We find that expressions of the radiated power, time-average stored electric energy, and time-average stored magnetic energy are similar to the mother impedance matrix of the VSIEs, where $\mathbf{J}_1\cdot\mathbf{J}_2^*$ is the multiplication of current basis functions and $(\nabla_1\cdot\mathbf{J}_1)\cdot(\nabla_2\cdot\mathbf{J}_2^*)$ is the multiplication of electric scalar potentials.

Table 1: Parameters of the antenna (all dimensions in mm).

L	W	W_1	L_1	R_1
10	10	1	3.5	2.5

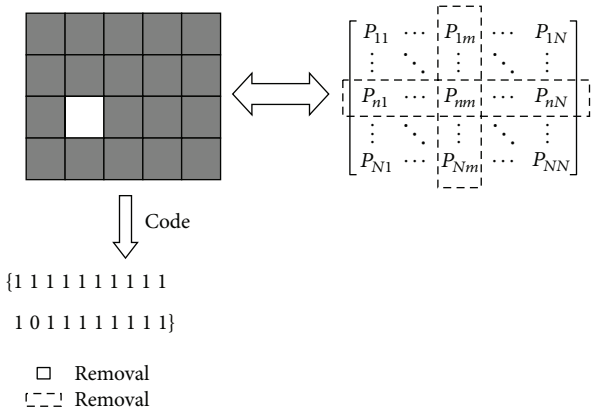

Figure 1: The rectangular mesh and the "mother" matrix.

When optimizing antenna bandwidth with the MoM, we usually determine the removal or retention of rows and columns in mother impedance matrix to achieve optimization goal. Similar "mother" matrices are computed at the same time for the stored electric and magnetic energies and radiated power. As shown in Figure 1, by optimizing antenna patch's shape, the rows and columns of removal are obtained, which will be removed in the radiated power matrix. After optimization, the matrix is multiplied by the coefficient of the surface current or electric displacement vector. Then the modules of all elements in matrix are in sum for computing the stored electric and magnetic energies and radiated power, which can easily obtain the Q value at a certain frequency point.

Cismasu and Gustafsson [25] have optimized a mobile terminal antenna, whose work is focused on narrow band. They do not compare antenna bandwidth before and after optimization. We extend this research on wideband antenna, which can shed light on design of wideband antennas.

4. Design of Wideband Antenna Based on Q Factor

With the above analysis, an antenna will be optimized. The topology of the racket shaped antenna is shown in Figure 2. The specific size of the antenna is shown in Table 1. The antenna is printed on a 10 mm × 10 mm × 0.5 mm PTFE substrate with a relative permittivity (ε_r) of 2.65. The antenna is fed by microstrip line, located at the bottom of the antenna. In order to extend antenna bandwidth, impedance matching technique will be used. As we know, charge will accumulate in abrupt structure, which increases the stored energy and results in reduction of antenna bandwidth. The stored energy will decrease in tapered structure, which will extend antenna bandwidth. The red arc gradient structure, generated by two ellipses, is employed between the microstrip line and the patch. The center of two ellipses is placed at coordinates (−1.5 mm, −3.5 mm, 0 mm) and (1.5 mm, −3.5 mm, 0 mm), respectively. Short axis, with a length of 1.2 mm, is in the X direction and long axis, with a length of 2.5 mm, is in the Y direction. Two ellipses connect to the circular patch well, which avoids the emergence of abrupt structure. The impedance matching method can gradually change the impedance along the transmission line to reduce the signal reflection [26].

In order to set the optimization goal, we need to study the current performance of the antenna first. The Q and S_{11} of the antenna before optimization are shown in Figures 6 and 7, respectively. The Q at the resonant frequency can be optimized directly to extend bandwidth for resonant antennas. However, as far as we know, for wideband antennas, there is no research on the optimization of Q. For this purpose, in this paper we consider combining Q factor with the MoM to optimize a wideband antenna. In order to ensure that the antenna bandwidth is as wide as possible, we conduct the optimization of the Q at a few frequency points to obtain the minimum of the sum of the Q, and the corresponding antenna will have the maximum bandwidth theoretically. Convex optimization [27], studied in some relevant literatures, can be well used in the optimization of Q. But it can only be used in the optimization of narrow band antennas as some mathematical treatments are correct only under the circumstance of narrow band antennas. In this paper, the DEA, which can be used under any circumstance, will be applied to optimize a wideband antenna.

It can be seen from Figures 6 and 7 that the antenna before optimization works in 11.5~16.5 GHz, and the Q of the antenna gradually decreases with the increase of frequency. Single Q has influence on factional bandwidth at resonant frequency. As the antenna is not a single-resonant antenna, we cannot use the single Q at resonant frequency point to calculate the fractional bandwidth. However, for the antenna in this paper, we have a comprehensive consideration of antenna Q within wideband. We can calculate the minimum of the sum of Q within its operating band to obtain maximum bandwidth.

In order to extend antenna bandwidth, we select 11 points between 11.5 GHz and 16.5 GHz with interval 0.5 GHz, and the sum of the Q at these 11 points is optimized to obtain the minimum, which can ensure antenna bandwidth is maximum. Therefore, the fitness function is defined as

$$X = \sum_{n=1}^{11} Q(n). \tag{18}$$

In order to facilitate the programming of MATLAB and the simulation of software, the patch and the ground plane of the antenna are divided into rectangular grids, which are encoded with 0 and 1. Zero represents removal of the grid and one represents retention of the grid. As each grid contains several triangles corresponding to some basis functions, removal or retention of these grids can be converted to removal or retention of basis functions. NP (the number of individuals) in (5) and T (the maximum generation) in (10) are all set to 20. In (9), D (length of code) is 148.

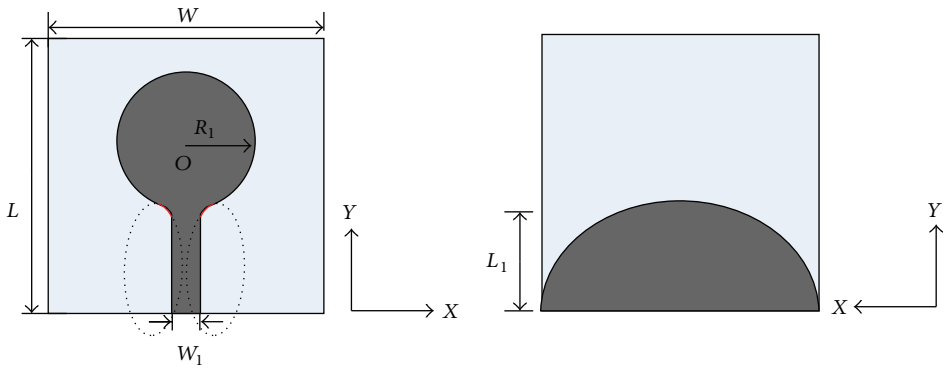

(a) Top view (b) Bottom view

Figure 2: Configuration of the antenna before optimization.

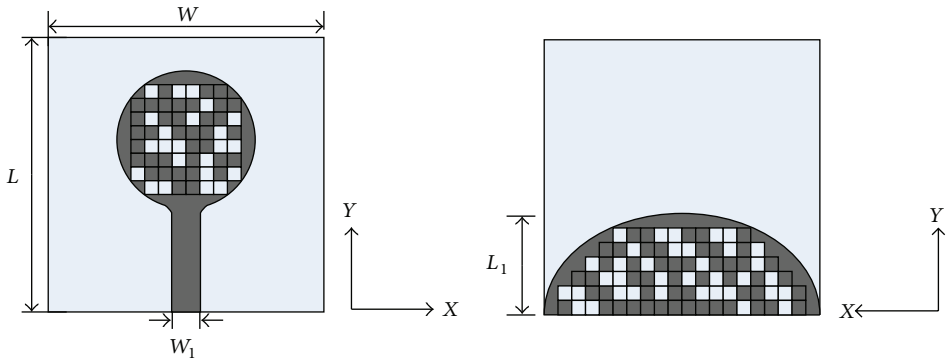

(a) Top view (b) Bottom view

Figure 3: Configuration of the optimized antenna.

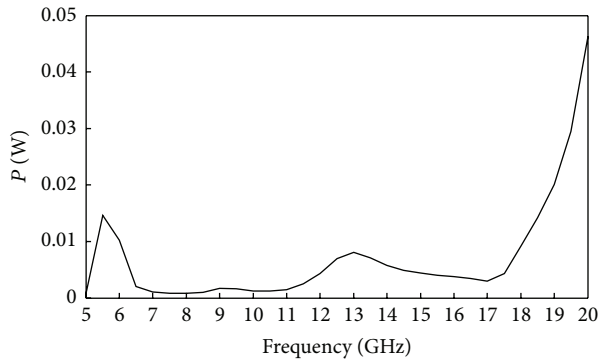

Figure 4: The radiated power of the optimized antenna.

The probability of removing grids is 0.4. In (6), the probability of each element in **F** choosing 1 or 0 is 0.5. The maximum and minimum cross factor in (10) conform to $CR_{max} = 0.35$ and $CR_{min} = 0.05$. The topology of the optimized antenna is shown in Figure 3. The radiated power and stored energy after optimization are shown in Figures 4 and 5, respectively. The Q and S_{11} before and after optimization are shown in Figures 6 and 7.

As can be seen from Figures 6 and 7, the Q of the antenna has greatly reduced and the bandwidth of the antenna has been extended from 11.5~16.5 GHz to 7~20 GHz. Assuming the optimized antenna is enclosed by the smallest circumscribing sphere, the Thal bound and McLean bound are given in Figure 6. We find that the optimized results are approaching the Thal bound and McLean bound but could not reach these bounds as the optimized antenna does not utilize the sphere volume efficiently.

To validate the simulated results, a prototype of the proposed antenna is fabricated. The fabricated prototype is shown in Figure 8. The measurements are conducted using Agilent N5230A PNA-L Network Analyzer. Figure 9 illustrates a comparison between the simulated and measured

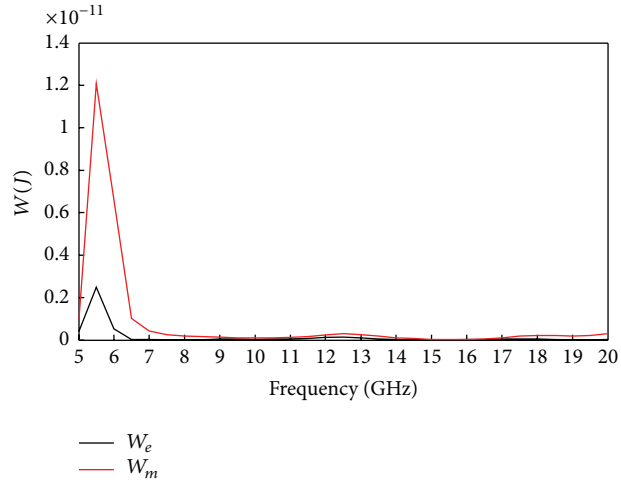

Figure 5: The stored energy of the optimized antenna.

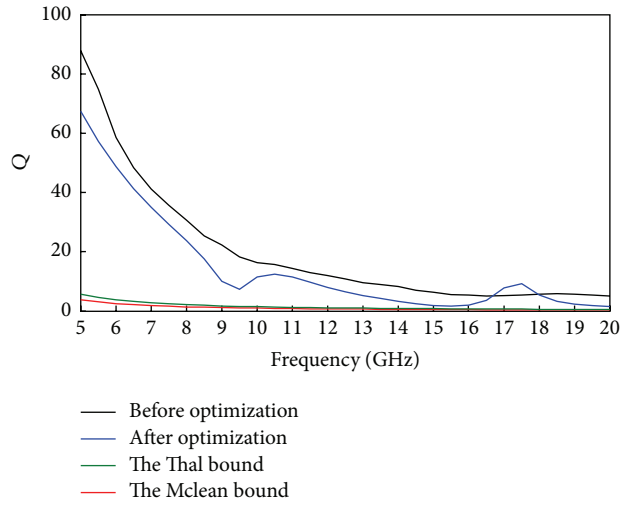

Figure 6: The Q of the antenna before and after optimization, the Thal bound, and the McLean bound.

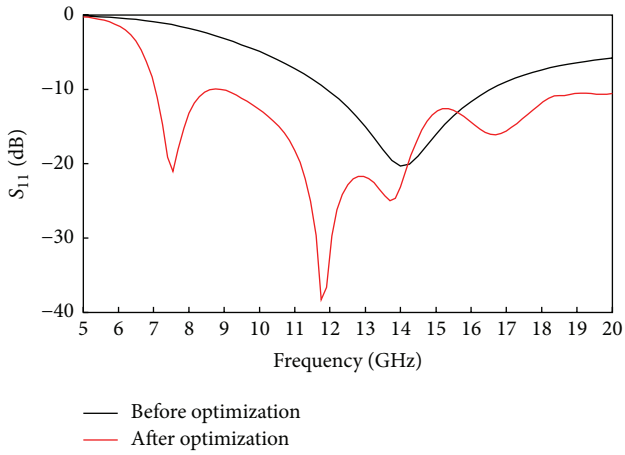

Figure 7: S_{11} of the antenna before and after optimization.

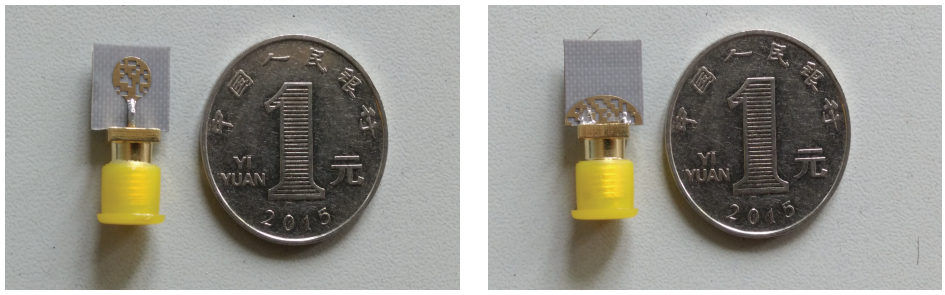

(a) Top view (b) Bottom view

Figure 8: Photograph of the fabricated antenna.

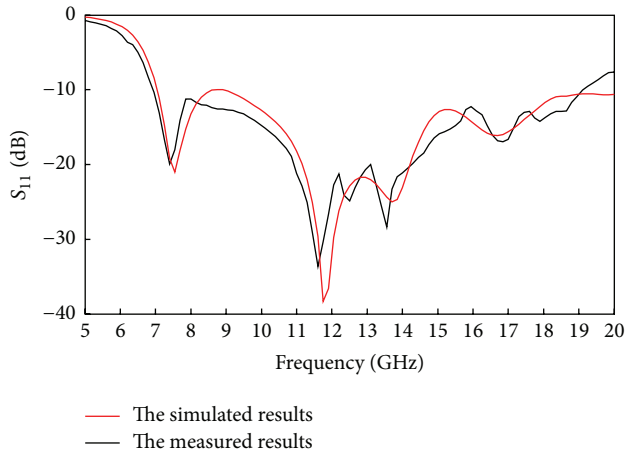

Figure 9: The simulated and measured S_{11} for the optimized antenna.

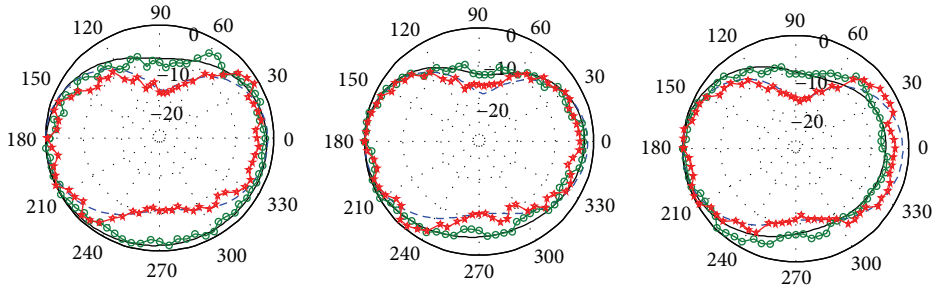

(a) 10 GHz (b) 14 GHz (c) 18 GHz

Figure 10: The simulated and measured far-field radiation patterns in E-plane and H-plane at different frequencies.

S_{11} of the proposed antenna with respect to frequency. From Figure 9 it can be observed that the simulated and measured results are in agreement. However, small discrepancies are present in the simulated and measured S_{11}. These discrepancies are associated with the substrate properties and fabrication tolerances. Also the use of the SMA connector in the measurements affects the operation of this electrically small antenna. A commercial level expert fabrication of the prototype would reduce these errors significantly. Overall, the bandwidth is achieved well by the antenna in simulation and in measurements.

We also measure the radiation patterns and peak gains of the proposed antenna in an anechoic chamber. The measured results are shown in Figures 10 and 11. As seen from Figure 10,

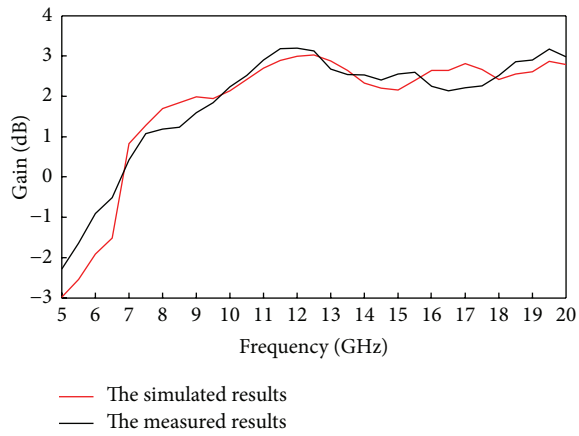

Figure 11: The simulated and measured peak gains of the proposed antenna.

the radiation patterns are close to omnidirectional in the *XOZ*-plane (*H*-plane) and "8" shape in the *YOZ*-plane (*E*-plane). Some discrepancies can be observed between the measured and simulated radiation patterns due to connector cables and misalignments. Figure 11 illustrates the variation of the measured and simulated peak gains with frequency. The antenna works properly as antenna gain is greater than 0 dB in 7~20 GHz.

5. Conclusion

In this paper, *Q* factor has been extended to the computation of wideband antennas. After that we combine *Q* factor and the VSIEs with adaptive DEA to optimize a planar microstrip antenna, which has extended the bandwidth from 11.5~16.5 GHz to 7~20 GHz and achieved a broadening rate of 160%. Computation of *Q* in previous work is feasible only on the condition of narrow band antennas. According to the best of the authors' knowledge, there is no literature indicating that *Q* can be applied to the computation of wideband antennas. Because the derivation of *Q* in this paper is not restricted to narrow band antennas, the computation of wideband antenna *Q* is also feasible. Therefore, the research in this paper can cast some new light on designing wideband antennas. Finally the antenna is fabricated and measured. The measured results have proven the correctness and effectiveness of the method.

Conflict of Interests

The authors declare that there is no conflict of interests regarding the publication of this paper.

References

[1] First Report and Order in the matter of Revision of Part 15 of the Commission's Rules Regarding Ultra-wideband Transmission Systems, Tech. Rep., 2002, https://apps.fcc.gov/edocs_public/attachmatch/FCC-02-48A1.pdf.

[2] P. B. Samal, P. J. Soh, and G. A. E. Vandenbosch, "UWB all-textile antenna with full ground plane for off-body WBAN communications," *IEEE Transactions on Antennas and Propagation*, vol. 62, no. 1, pp. 102–108, 2014.

[3] Y.-J. Ou, F. Yang, Z.-P. Nie, and Z.-Q. Zhao, "Designs of single layer broadband microstrip antennas using genetic algorithm," *Chinese Journal of Radio Science*, vol. 23, no. 3, pp. 434–437, 2008.

[4] J. Kim, T. Yoon, J. Kim, and J. Choi, "Design of an ultra wideband printed monopole antenna using FDTD and genetic algorithm," *IEEE Microwave and Wireless Components Letters*, vol. 15, no. 6, pp. 395–397, 2005.

[5] S. C. D. Barrio, A. Morris, and G. F. Pedersen, "Antenna miniaturization with MEMS tunable capacitors: techniques and trade-offs," *International Journal of Antennas and Propagation*, vol. 2014, Article ID 709580, 8 pages, 2014.

[6] H.-Y. Li, C.-C. Lin, T.-K. Lin, and C.-Y. Huang, "Low-profile folded-coupling planar inverted-F antenna for 2.4/5 GHz WLAN communications," *International Journal of Antennas and Propagation*, vol. 2014, Article ID 182927, 7 pages, 2014.

[7] T. Yu and C. Y. Yin, "Full-wave analysis of microstrip antennas in three-layered spherical media," *International Journal of Antennas and Propagation*, vol. 2013, Article ID 298538, 8 pages, 2013.

[8] S. N. Makarov, *Antenna and EM Modeling with MATLAB*, Beijing University of Posts and Telecommunications Press, Beijing, China, 2006.

[9] A. K. Qin, X. Li, H. Pan, and S. Xia, "Investigation of self-adaptive differential evolution on the CEC-2013 real-parameter single-objective optimization testbed," in *Proceedings of the IEEE Congress on Evolutionary Computation (CEC '13)*, pp. 1107–1114, Cancún, México, June 2013.

[10] R. Zhang, H. Gao, and T. Zhang, "Hybrid optimization algorithm based on quantum and differential evolution for continuous space optimization," *Systems Engineering and Electronics*, vol. 34, no. 6, pp. 1288–1292, 2012.

[11] A. Glotic, A. Glotic, P. Kitak, J. Pihler, and I. Ticar, "Parallel self-adaptive differential evolution algorithm for solving short-term hydro scheduling problem," *IEEE Transactions on Power Systems*, vol. 29, no. 5, pp. 2347–2358, 2014.

[12] "Physical limitations of omnidirectional antennas," Tech. Rep., 1948, http://m.doc88.com/p-9075757608767.html.

[13] R. F. Harrington, "Effect of antenna size on gain, bandwidth, and efficiency," *Journal of Research of the National Bureau of Standards D: Radio Propagation*, vol. 64, no. 1, pp. 1–12, 1960.

[14] J. S. McLean, "A re-examination of the fundamental limits on the radiation Q of electrically small antennas," *IEEE Transactions on Antennas and Propagation*, vol. 44, no. 5, pp. 672–676, 1996.

[15] H. C. Huang, X. Xu, and Y. E. Wang, "Dual-band isotropic radiation patterns from a printed electrically small loop-loaded dipole antenna," in *Proceedings of the IEEE International Symposium on Antennas and Propagation and USNC/URSI National Radio Science Meeting (APSURSI '09)*, North Charleston, SC, USA, June 2009.

[16] H. L. Thal Jr., "New radiation Q limits for spherical wire antennas," *IEEE Transactions on Antennas and Propagation*, vol. 54, no. 10, pp. 2757–2763, 2006.

[17] L. Jelinek, M. Capek, P. Hazdra, and J. Eichler, "An analytical evaluation of the quality factor Q_Z for dominant spherical modes," *IET Microwaves, Antennas & Propagation*, vol. 9, no. 10, pp. 1096–1103, 2015.

[18] A. D. Yaghjian, "Improved formulas for the Q of antennas with highly lossy dispersive materials," *IEEE Antennas and Wireless Propagation Letters*, vol. 5, no. 1, pp. 365–369, 2006.

[19] L. Sun, M. He, J. Hu, Y. Zhu, and H. Chen, "A butterfly-shaped wideband microstrip patch antenna for wireless communication," *International Journal of Antennas and Propagation*, vol. 2015, Article ID 328208, 8 pages, 2015.

[20] L. Damaj, A. C. Lepage, and X. Begaud, "A compact wideband dual-polarized antenna with harmonic suppression using non-uniform defected ground structure," *International Journal of Antennas and Propagation*, vol. 2015, Article ID 505123, 7 pages, 2015.

[21] A. D. Yaghjian and S. R. Best, "Impedance, bandwidth, and Q of antennas," *IEEE Transactions on Antennas and Propagation*, vol. 53, no. 4, pp. 1298–1324, 2005.

[22] G. A. E. Vandenbosch, "Reactive Energies, impedance, and Q factor of radiating structures," *IEEE Transactions on Antennas and Propagation*, vol. 58, no. 4, pp. 1112–1127, 2010.

[23] A. K. Rashid and Z. Shen, "On the inverse relationship between quality factor and bandwidth of small antennas," in *Proceedings of the Asia Pacific Microwave Conference (APMC '09)*, pp. 44–47, Singapore, December 2009.

[24] M. Capek, L. Jelinek, and P. Hazdra, "On the functional relation between quality factor and fractional bandwidth," *IEEE Transactions on Antennas and Propagation*, vol. 63, no. 6, pp. 2787–2790, 2015.

[25] M. Cismasu and M. Gustafsson, "Illustration of mobile terminal antenna optimization by genetic algorithms with single frequency simulation," in *Proceedings of the 21st International Symposium on Electromagnetic Theory (EMTS '13)*, pp. 84–87, IEEE, Hiroshima, Japan, May 2013.

[26] J. Wu, Z. Zhao, Z. Nie, and Q.-H. Liu, "A printed UWB vivaldi antenna using stepped connection structure between slotline and tapered patches," *IEEE Antennas and Wireless Propagation Letters*, vol. 13, pp. 698–701, 2014.

[27] J. Pan and J.-J. Zhou, "Khatri-Rao subspace wideband DOA estimation based on convex optimization," *Journal of Electronics and Information Technology*, vol. 35, no. 1, pp. 80–84, 2013.